

Chain-Length Dependence of Termination Rate Coefficients in Acrylate and Methacrylate Homopolymerizations Investigated via the SP–PLP Technique

Michael Buback, Mark Egorov,* and Achim Feldermann

*Institute of Physical Chemistry, University of Goettingen,
Tammannstrasse 6, 37077 Goettingen, Federal Republic of Germany*

Received July 28, 2003; Revised Manuscript Received December 15, 2003

ABSTRACT: Termination rate coefficients, k_t , of alkyl acrylate and alkyl methacrylate homopolymerizations at 40 °C and pressures of 1000 and 2000 bar have been measured up to high degrees of monomer conversion using the time-resolved single-pulse–pulsed-laser polymerization (SP–PLP) technique. The chain-length dependence (CLD) of k_t has been deduced from SP–PLP data by adopting the power-law model, $k_t = k_t^0 i^{-\alpha}$, where i is the chain length. For methacrylates at low degrees of monomer conversion, α is close to the theoretically predicted value of 0.16. At conversions above 20% the exponent α increases significantly with increasing conversion. This effect becomes particularly pronounced in the gel effect region, where α , e.g. for MMA, reaches values close to unity. In the case of acrylates with small alkyl ester side chain, such as methyl acrylate, α is also close to 0.16 at low conversions and increases toward higher conversions. In the case of acrylates with larger alkyl ester side chain, such as dodecyl acrylate and 2-ethylhexyl acrylate, however, α is close to 0.4 even at low degrees of monomer conversion. The latter effect is strongly indicative of intramolecular chain transfer, which generates significant amounts of midchain radicals in the system. The fact that such transfer processes take place is supported by SP–PLP data on alkyl acrylates polymerized in mixtures with supercritical carbon dioxide.

1. Introduction

Knowledge of rate coefficients of propagation and termination in free-radical polymerization (FRP) is essential for both the understanding of the fundamental kinetics of the process and the design of technical polymerizations.¹ Propagation is chemically controlled in an extended conversion range, so the propagation rate coefficient, k_p , is independent of the physical properties of the polymerizing medium, such as viscosity, up to fairly high degrees of monomer conversion. That is why k_p values measured at low conversion via the PLP–SEC (pulsed-laser polymerization–size-exclusion chromatography) technique,² recommended by IUPAC,³ apply over a wide range of monomer conversions. The determination of the termination rate coefficient, k_t , is much more demanding from both a theoretical and an experimental point of view because the reaction of radical–radical termination is diffusion-controlled from the very beginning of polymerization. k_t may vary with the physical properties of the reacting free-radical species, e.g., with their chain length (CL) and their branching characteristics. Moreover, the physical properties of the medium, e.g., polymer concentration or the amount and quality of a solvent, may also play an important role.⁴

Only a few experimental methods for measuring the CL and conversion dependence of k_t have been put forward so far.⁵ Laser-based techniques are particularly advantageous as they enable an independent study of the variation of k_t with monomer conversion and radical chain length. Among them, the single-pulse–pulsed-laser polymerization (SP–PLP) technique is very attractive as it allows for measuring k_t over a wide range of monomer conversions. This method was developed for studying the kinetics of ethene polymerization⁶ and

since then has been widely used for investigations into the termination kinetics of acrylate and methacrylate polymerizations in bulk and in solution at various temperatures and pressures.^{7–9} However, the potential of the SP–PLP method with respect to any detailed studies into the dependence of k_t on free-radical chain length has not been fully explored so far. The present work focuses on this aspect.

The idea of the SP–PLP method is as follows. A monomer–photoinitiator mixture is placed in an optical (high-pressure) cell of transmission type with two windows that are transparent in the spectral range from visible to IR frequencies. Primary radicals are generated using an excimer laser pulse of about 20 ns duration. These primary radicals from photoinitiator decomposition (initiator-derived radical species) then start free-radical growth (polymerization) by adding monomer molecules. The resulting pulse-induced change in monomer conversion, usually from 0.01 up to a few percent, is monitored with a time resolution of microseconds via online near-IR spectroscopy. So far, most of the SP–PLP experiments have been carried out at elevated or high pressure. Application of pressure enhances the propagation rate and slows down the termination rate. This results in a larger pulse-induced monomer conversion, which is associated with an improved SP–PLP signal-to-noise quality. The monomer conversion vs time trace yields the ratio of CL-averaged overall k_t to k_p , $\langle k_t \rangle / k_p$. With k_p being independently determined via PLP–SEC, $\langle k_t \rangle / k_p$ provides access to $\langle k_t \rangle$ values. As will be shown, model-based analysis of an SP–PLP trace may also provide information on the CLD of k_t in terms of the quantity $k_t(i, j)$. The notation $k_t(i, j)$ indicates that under conditions of negligible chain transfer termination occurs between two free radicals of (almost) identical size i . Both $\langle k_t \rangle$ and $k_t(i, j)$ may be determined for a wide range of monomer conversions from individual SP–PLP

* Corresponding author: e-mail megorov@gwdg.de.

experiments carried out during the course of a polymerization reaction.

In our previous work we presented general mathematical expressions for deducing k_t from SP–PLP data for different termination models. Side effects, such as chain transfer to monomer and nonsymmetric initiator decomposition into two primary radical species of quite different activity toward monomer addition, were also considered.¹⁰ These expressions, however, have too many parameters, which significantly hinders the analysis of SP–PLP data. This problem may be circumvented by carrying out an SP–PLP experiment under close-to-ideal conditions. In that case simpler expressions for data analysis may be used. A perfect SP–PLP experiment requires that both free-radical species from photoinitiator decomposition readily add to monomer to start macromolecular growth. α -Methyl-4-(methylmercapto)- α -morpholinopropiophenone (MMMP) meets this requirement. Moreover, MMMP is well-soluble in most of the common monomers. That MMMP decomposes into two propagating primary radicals has also been demonstrated through electron spray ionization (ESI) experiments by the Davis group.¹¹ DMPA (2,2-dimethoxy-2-phenylacetophenone), which has been used in previous studies as the photoinitiator, is nonideal in that it decomposes into two fragments one of which does not add to monomer but primarily reacts with free radicals and thus acts as an inhibitor.¹² This has been demonstrated via PREDICI simulations^{10,13} and by ESI analysis.¹⁴

If monomer conversion per pulse is too small, as with methacrylates, where it may be less than 0.01%, a sequence of laser pulses is applied to the monomer–photoinitiator mixture, and the resulting signals are co-added. By this procedure the signal-to-noise ratio is significantly enhanced. Because of a better quality of SP–PLP signals, one can now analyze SP–PLP data in the initial time region after the pulse where chain transfer to monomer is negligible. In this initial time region the primary free radicals generated at $t = 0$ grow at the same rate, with their chain length i increasing linearly with time t after the pulse. Thus, the size distribution of free radicals is narrow (of Poisson type), and at a given moment in time, the overall k_t is equal to the individual (or microscopic) termination rate coefficient, $k_t(i, i)$. SP–PLP experiments thus provide access to measuring the chain-length dependence of k_t .¹⁵ A mathematical procedure for deriving the CLD of k_t from an ideal SP–PLP experiment will be outlined in section 3. Recent experimental results will be presented and discussed in section 4.

2. Experimental Section

The SP–PLP experiments were carried out as described elsewhere.¹⁶ The photoinitiator α -methyl-4-(methylmercapto)- α -morpholinopropiophenone (MMMP, 98%, Aldrich Chemie) was used as supplied at initial concentrations close to 1×10^{-2} mol L⁻¹. Methyl acrylate (>99%, stabilized with 0.005 wt % hydroquinone monomethyl ether, Fluka Chemie), butyl acrylate (>99%, stabilized with 0.005 wt % hydroquinone monomethyl ether, Fluka Chemie), dodecyl acrylate (which actually is a mixture of 55 wt % DA and 45 wt % tetradecyl acrylate, Fluka Chemie), methyl methacrylate (>99%, stabilized with 0.005 wt % hydroquinone monomethyl ether, Fluka Chemie), dodecyl methacrylate (DMA, \approx 96%, Aldrich Chemie), 2-ethylhexyl acrylate (>98%, Fluka), and n -hexyl acrylate (>95%, Lancaster) were purified by distillation under reduced pressure in the presence of K₂CO₃ and treated by several freeze–pump–thaw cycles to remove dissolved oxygen. The samples were

irradiated with XeF excimer laser pulses (at 351 nm) of 2–3 mJ incident energy per pulse. Laser-induced monomer conversion was monitored via online near-IR spectroscopy. For this purpose, the first overtone of the C–H vibration of carbon atoms engaged in a C=C double bond absorbing at around 6170 cm⁻¹ was used. After applying a series of excimer laser pulses, each being followed by microsecond time-resolved near-IR spectroscopic measurement of pulse-induced polymerization, the reaction cell was inserted into the sample chamber of an IFS 88 Fourier transform IR/NIR spectrometer (Bruker) where absolute monomer concentration was checked. During each polymerization experiment, SP–PLP measurements were carried out until the reacting system became inhomogeneous or the photoinitiator was consumed. The occurrence of inhomogeneity was established by visual inspection and/or by observing a pronounced shift of the baseline in the NIR spectra. (In this case also the shape of the SP–PLP signal becomes very irregular.) Within the present work, all the SP–PLP experiments were carried out at 40 °C and 1000 bar (except for MMA which, in addition, was polymerized at 40 °C and 2000 bar) up to high degrees of monomer conversion; e.g., in some cases conversions just below 70% were reached.

3. Termination Rate Coefficients from SP–PLP

The rate of polymerization, r_p , in ideal free-radical polymerization is defined by the following expression:

$$r_p \equiv -\frac{dc_M}{dt} = k_p c_M c_R \quad (1)$$

where c_M and c_R are monomer and overall free-radical concentration, respectively, and t is polymerization time. Under conditions of single-pulse initiation, the rate of termination, r_t , is given by

$$r_t \equiv -\frac{dc_R}{dt} = 2k_t c_R^2 \quad (2)$$

where $k_t = k_t^c + k_t^d$ is the overall termination rate coefficient, with k_t^c and k_t^d being the rate coefficients of termination by combination and disproportionation, respectively. (In what follows we consider the specific situation which occurs in pulsed-laser polymerization; i.e., we assume that primary radicals are generated instantaneously at $t = 0$ by applying a laser pulse to a monomer–photoinitiator mixture.) The factor of “2” has been introduced into eq 2 and into all the relevant equations throughout the present work in accordance with the IUPAC preferred definition of k_t .⁴

Under condition of negligible chain transfer radicals generated at $t = 0$ grow at the same rate so that chain lengths of growing radicals are more or less identical at any given moment of time t after the pulse. In that case, free-radical chain length i is proportional to the time of radical growth (after applying the laser pulse) so that

$$i = k_p c_M t = \Theta t \quad (3)$$

where $\Theta = k_p c_M$ is the propagation rate of a single radical. The above expression holds for times $t < t_{tr}$, where $t_{tr} = (k_{tr} c_M)^{-1}$ is the time after which, on average, chain transfer to monomer occurs. t_{tr} is about 0.1 s for acrylates and about 1.0 s for methacrylates (under the chosen experimental conditions). These estimates have been obtained assuming that the dimensionless constant of chain transfer to monomer is 10^{-5} for both acrylates and methacrylates and that typical k_p values for acrylates and methacrylates at 40 °C and 1000 bar are 30 000 and 1500 L mol⁻¹ s⁻¹, respectively (see Table 1). The

Table 1. Kinetic Parameters Used for SP–PLP Model Calculations

monomer	k_p (L mol ⁻¹ s ⁻¹)	c_M^0 (mol L ⁻¹) ^e	$\log(k_t^0/(L mol^{-1} s^{-1}))$ (up to 15% conv)	α (up to 15% conv)
MMA	1 700 ^{a,b}	10.1	7.6	0.14
DMA	1 400 ^b	3.6	6.4	0.11
MA	28 600 ^b	11.8	8.3	0.15
BA	35 600 ^b	7.2	7.8	0.14
DA	39 800 ^b	3.6	7.9	0.42
<i>n</i> -hexyl acrylate	38 000 ^c	5.7	8.2	0.29
2-ethylhexyl acrylate	38 000 ^c	4.8	8.1	0.45
BA in scCO ₂	24 900 ^d	4.6	9.0	0.35
DA in scCO ₂	30 200 ^d	2.4	8.6	0.42

^a 40 °C/2000 bar. ^b Literature data (see refs 2 and 3). ^c Estimated value. ^d Literature data (see refs 33 and 34). ^e Monomer density at zero conversion divided by (monomer) molecular weight.

analysis of chain-length-dependent k_t has been restricted to this initial time region where the free-radical size distribution after each pulse is monodisperse (of Poisson type) and is linearly correlated with t unless other transfer reactions, e.g., intramolecular transfer to polymer such as backbiting, start to dominate the kinetics.

De Kock's Approach and the Second-Derivative Problem. Equations 1–3 allow for deducing simple expressions which relate k_t either to monomer concentration as a function of time or to the number chain-length distribution of produced polymer. For example, from eqs 1 and 2 one can easily obtain eq 4, which relates individual k_t to time-resolved monomer concentration, $c_M(t)$:

$$k_t = \frac{k_p}{2} \left\{ \frac{\ddot{c}_M c_M}{\dot{c}_M^2} - 1 \right\} \quad (4)$$

where $\dot{c}_M \equiv dc_M/dt$ and $\ddot{c}_M \equiv d^2c_M/dt^2$.¹⁷ It should be noted that eq 4 is also valid under conditions of strong chain transfer (to monomer).

Equation 4 implies that, under SP–PLP conditions, k_t is a function of time t after the laser pulse. In the absence of chain transfer (to monomer) processes, the variation of k_t with time is equivalent to the variation of microscopic (individual) termination rate coefficients $k_t(i, t)$ with chain length: $k_t = k_t(i, t)$.

At longer times after the pulse, chain transfer to monomer may no longer be ignored, and the macroscopic termination rate coefficient, k_t , deduced from eq 4, will become some chain-length-averaged coefficient. To extract information on $k_t(i, t)$ from SP–PLP experimental data, one has to use a more general expression for k_t .¹⁰

The method based on eq 4 is model-free. The only parameter that needs to be known is k_p , which may be measured via PLP–SEC. With other methods, additional parameters, such as initial radical concentration or the quantity δ characterizing the contribution of disproportionation to overall termination, must be known as well.¹⁷ The main disadvantage associated with de Kock's approach is the requirement of a twofold differentiation of monomer concentration data, $c_M(t)$ (see eq 4). The quality of time-resolved SP–PLP data, at least at present, is not sufficient for reasonably carrying out such differentiation. For this reason, methods based on a particular termination model are usually employed. k_t is determined by fitting an expression for $c_M(t)$ derived for a given termination model to SP–PLP experimental data.

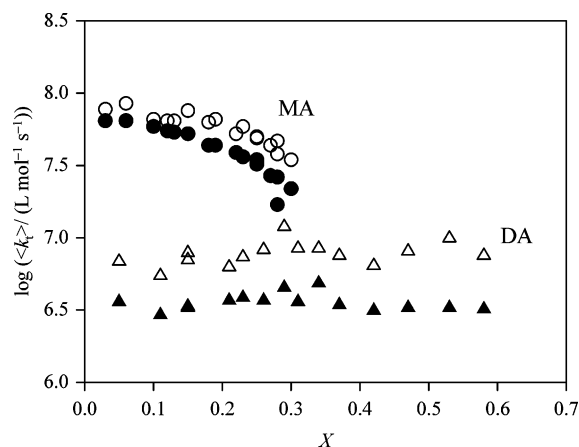


Figure 1. Dependence of $\log \langle k_t \rangle$ on monomer conversion, X , for bulk homopolymerizations of MA (\circ , \bullet) and DA (\triangle , \blacktriangle) at 1000 bar and 40 °C. $\langle k_t \rangle$ values were obtained by fitting eq 5 to SP–PLP data in the time intervals $0 < t < 0.02$ s (open symbols) and $0 < t < 0.1$ s (full symbols).

Ideal Kinetics Model. Before using any model that takes CLD of k_t into account, one should show that ideal kinetics cannot adequately describe the SP–PLP data. The easiest way to demonstrate that is to fit an expression deduced for constant k_t , eq 5, to an SP–PLP trace taking different time intervals for analysis.

$$\frac{c_M(t)}{c_M^0} = (1 + 2\langle k_t \rangle c_R^0 t)^{-k_p/(2\langle k_t \rangle)} \quad (5)$$

where c_M^0 and c_R^0 are the monomer and the radical concentrations at time $t = 0$, respectively. Equation 5 was derived by substituting eq 1 into eq 2 and then integrating it. This equation describes laser-induced monomer concentration, $c_M(t)$, as a function of time after firing the laser at $t = 0$. In the case of chain-length-independent k_t and k_p , identical rate parameters, e.g., $\langle k_t \rangle/k_p$, should result irrespective of the time range of an SP–PLP trace that is subjected to the fitting procedure.

The fitting of eq 5 to SP–PLP data yields two parameters, $\langle k_t \rangle/k_p$ and $\langle k_t \rangle c_R^0$. As k_p is available from independent PLP–SEC experiments,^{2,3} $\langle k_t \rangle$ may be immediately obtained from $\langle k_t \rangle/k_p$.

Figure 1 shows conversion-dependent k_t values for bulk homopolymerizations of methyl acrylate (MA, circles) and dodecyl acrylate (DA, triangles) at 1000 bar and 40 °C obtained by fitting eq 5 to SP–PLP data in a short ($0 < t < 0.02$ s, open symbols) and a long ($0 < t < 0.1$ s, full symbols) time interval, respectively. Both time regions are, however, within the range $t < t_{tr}$. As can be seen, k_t values for shorter times and thus for shorter chains (open symbols) lie above the associated numbers obtained by fitting eq 5 to the same SP–PLP trace but over a more extended time range (full symbols). The differences are minor for MA at low and moderate degrees of monomer conversion but become more pronounced toward high conversions. For DA significant differences in $\langle k_t \rangle$ are seen throughout the entire monomer conversion range. The data in Figure 1 provide clear evidence for k_t decreasing with free-radical chain length.

Figure 2a shows the conversion dependence of $\langle k_t \rangle$ for methyl methacrylate (MMA). Corresponding data for dodecyl methacrylate (DMA) are presented in Figure 2b.

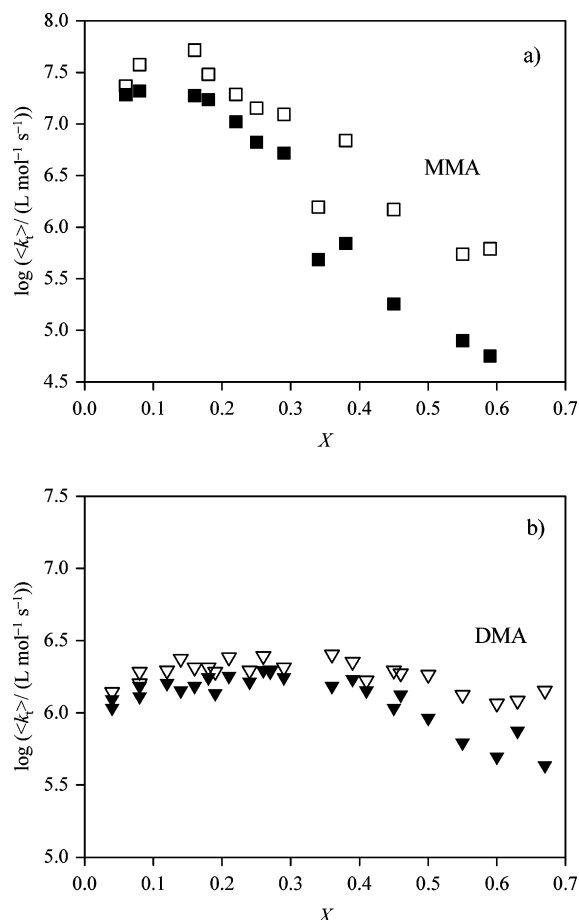


Figure 2. Dependence of $\log \langle k_t \rangle$ on monomer conversion, X , for bulk homopolymerizations of (a) MMA (\square , \blacksquare) and (b) DMA (∇ , \blacktriangledown) at 1000 bar and 40 °C. $\langle k_t \rangle$ values were obtained by fitting eq 5 to SP–PLP data in the time intervals $0 < t < 0.1$ s (open symbols) and $0 < t < 0.5$ s (full symbols).

The results shown in Figure 2a,b are from SP–PLP experiments carried out at 40 °C and 1000 bar. The open symbols represent the results of fitting eq 5 to SP–PLP data in the time interval $0 < t < 0.1$ s, whereas the full symbols refer to fits over a longer time interval, $0 < t < 0.5$ s. In the case of MMA the difference between the $\langle k_t \rangle$ values referring to short and long time intervals of the same SP–PLP trace (and thus to short and long average chain lengths) is small at low degrees of monomer conversion but becomes significant at conversions above 20%, where also absolute $\langle k_t \rangle$ clearly changes. With DMA, the difference between the $\langle k_t \rangle$ s for short and long chains is weak at low conversions. Toward higher degrees of monomer conversion this difference increases but to a much smaller extent than with MMA.

Another observation that can be made from Figures 1 and 2 is that $\langle k_t \rangle$ s for DA and for DMA are more or less constant up to about 70% conversion, whereas $\langle k_t \rangle$ for MMA, above 20% monomer conversion, is significantly reduced upon further polymerization. The decrease in MMA $\langle k_t \rangle$ by about 3 orders of magnitude below the initial plateau value (up to 20% monomer conversion) suggests that different diffusion mechanisms are dominant at low and at moderately high conversions.¹⁸

The results shown in Figures 1 and 2 may be summarized as follows: k_t clearly decreases with increasing chain length. The size of this effect, however, varies with the type of monomer and with monomer conversion.

Power-Law Model for Chain-Length-Dependent k_t . Figures 1 and 2 evidently show that k_t is chain-length-dependent. The quantitative analysis of SP–PLP traces thus requires an expression which takes CLD of k_t explicitly into account. The most widely used such expression is the so-called power-law model,^{19,20} which assumes k_t to vary with free-radical chain length i according to

$$k_t(i, t) = k_t^0 i^{-\alpha} \quad (6)$$

where k_t^0 is the termination rate coefficient for very small free radicals and i is radical chain length. Equation 6 assumes that chain transfer to monomer may be neglected. The terminating radicals thus are of identical length. Using eq 6 and eqs 1–3, one may derive the following expressions for overall free-radical concentration and rate of polymerization, respectively:

$$c_R \cong c_R^0 \left(1 + \frac{2c_R^0 k_t^0}{(1-\alpha)\Theta^\alpha} t^{1-\alpha} \right)^{-1} \quad (7)$$

$$\frac{dc_M}{dt} \cong -\Theta c_R^0 \left(1 + \frac{2c_R^0 k_t^0}{(1-\alpha)\Theta^\alpha} t^{1-\alpha} \right)^{-1} \quad (8)$$

Integration of eq 8 yields the following integral expression for relative monomer concentration $c_M(t)/c_M^0$ (see refs 10 and 15):

$$\frac{c_M(t)}{c_M^0} = 1 - \frac{b}{c} \int_0^t (b \int_0^{t'} (t_p/t')^\alpha dt'' + 1)^{-1} dt' \quad (9)$$

with $b \equiv 2c_R^0 k_t^0$ and $c \equiv 2k_t^0/k_p$. $t_p = (k_p c_M^0)^{-1}$ is the time required for the first propagation step (and, to good approximation, is also the time required for each subsequent propagation step, as $c_M \cong c_M^0$). Fitting eq 9 to an SP–PLP trace yields k_t^0/k_p , $c_R^0 k_t^0$, and α . Such fitting can be carried out using, for example, the software package Origin Professional v. 6.1.

Other Models for Chain-Length-Dependent k_t . It goes without saying that beyond the power-law model also other termination models may be used for k_t analysis of SP–PLP traces. One may, for example, consider the following termination model which has been discussed in detail in ref 10:

$$k_t(i, t) = k_t^0 \omega(i), \quad \omega(i) = \begin{cases} 1, & i < i_e \\ (i_e/i)^{3/2}, & i > i_e \end{cases} \quad (10)$$

where i_e is the so-called entanglement length. The exponent $3/2$, predicted by de Gennes,²¹ accounts for the diffusion of long (entangled) radicals in semidilute or concentrated polymer solutions. A more general expression for chain-length-dependent k_t reads

$$k_t(t) = k_t^0 \omega(t), \quad \omega(t) = \omega_{RD} + \begin{cases} (t_p/t)^\alpha, & t_p < t < t_e \\ (t_p/t_e)^\alpha (t_e/t)^\gamma, & t > t_e \end{cases} \quad (11)$$

where t_e is the time at which the radicals reach the entanglement length i_e and ω_{RD} is the ratio of $k_{t, RD}/k_t^0$, with $k_{t, RD}$ being the reaction diffusion coefficient.¹⁸ Equation 11 rests on the assumption that free-radical chain length increases linearly with time t after the

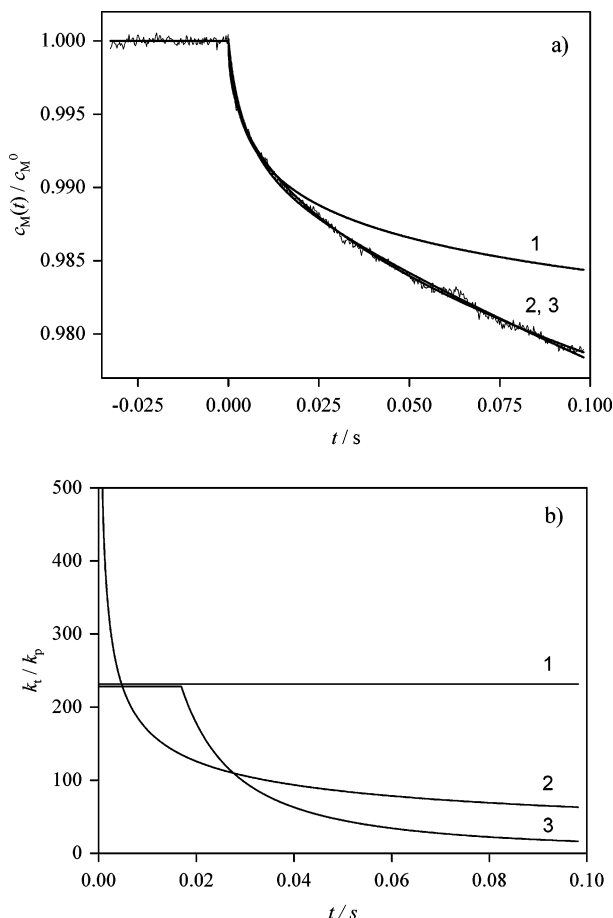


Figure 3. SP-PLP trace for DA at 1000 bar and 40 °C (a). DA conversion from preceding polymerization is 11%. The solid lines are results of fitting eq 12 to the SP-PLP data for three different termination models: ideal kinetics model ($k_t = \text{constant}$), with eq 12 fitted to the data in the time interval from $t = 0$ to $t = 0.02$ s (curve 1); power-law model, eq 6 (curve 2); and the model given by eq 10 (curve 3). Curves 2 and 3 are fits to the entire signal from $t = 0$ to 0.1 s. The time dependence of k_t/k_p for the above-mentioned models is illustrated in (b).

laser pulse (see eq 3). The exponents α ($\alpha < 0.5$) and γ ($\gamma > 1$) account for the diffusion of short (nonentangled) and long-chain (entangled) radicals, respectively. Obviously, eqs 6 and 10 are specific cases of eq 11; e.g., eq 6 is obtained from eq 11 by setting $\gamma = 0$ and $t_e \rightarrow \infty$.

For the termination model represented by eq 11, the relative change in monomer concentration after the laser pulse will be given by the following integral expression:

$$\frac{c_M(t)}{c_M^0} = 1 - \frac{b}{c} \int_0^t (b \int_0^{t'} \omega(t'') dt'' + 1)^{-1} dt' \quad (12)$$

Equation 12 may be fitted to SP-PLP data to yield the values of the parameters b , c , α , γ , i_e , and $k_{t, \text{RD}}$.²²

Model Discrimination. Figure 3a shows an SP-PLP trace measured for DA at 40 °C, 1000 bar, and 11% initial monomer conversion (from preceding polymerization). Curve 1 in Figure 3a was obtained by fitting the ideal kinetic model, eq 5, to the initial 20% of the $c_M(t)$ trace, $0 < t < 0.02$ s, and using the so-obtained fit parameters to draw a curve for the entire time interval, i.e., up to 0.1 s. Curves 2 and 3 are fits of eq 12 to the data for the models represented by eqs 6 and 10, respectively. As can be seen, curves 2 and 3, although

referring to quite different termination models (illustrated in Figure 3b), equally well describe the experimental data. This observation is fully supported by comparison of the minimized χ^2 values obtained from fitting the two models to the data using Origin.²³ The same holds true for DA at other degrees of monomer conversion and for the other monomers of the present study.

Even though SP-PLP provides clear evidence of k_t decreasing with CL, the SP-PLP technique does not allow for elucidation of the detailed mechanism of chain-length-dependent termination. In what follows, the power-law expression, eq 6, will be used, primarily because of its simplicity but also because of existing theoretical predictions for the power-law exponent α . The resulting parameters, α and k_t^0 , obviously are model-dependent kinetic parameters. Nevertheless, they should be useful for quantitative analysis of the chain-length dependence of k_t for different systems at different conversions.

4. Analysis of SP-PLP Data Using the Power-Law Model

The presentation and discussion of results will be subdivided into an acrylate and a methacrylate part. The reason behind this separation is that PLP-SEC studies directed toward measuring k_p (by size-exclusion chromatography carried out on polymer samples produced by periodic laser pulse initiation) indicated special problems occurring with acrylates. Some of these problems are due to intramolecular chain transfer, e.g., via backbiting. The associated difficulties may also affect the analysis of SP-PLP data. The data for methacrylates will be analyzed first. Because the α -hydrogen atoms of acrylates are replaced by methyl groups, free radicals occurring in methacrylate polymerizations are less reactive. As a consequence, easily abstractable hydrogen atoms are not available. The analysis of SP-PLP of methacrylates should therefore be somewhat easier, although the quality of SP-PLP signals for methacrylates is generally lower than that for acrylates because of a significantly lower k_p of methacrylates as compared to acrylates.

SP-PLP of Alkyl Methacrylates. Plotted in parts a and b of Figure 4 are the values of α and k_t^0 , respectively, obtained by fitting eq 9 to SP-PLP data for MMA and DMA. Kinetic parameters used for SP-PLP model calculations are summarized in Table 1.

The value of the exponent α scatters around 0.16 for both monomers at conversions below 20%, that is, in the initial "plateau" region of almost constant overall $\langle k_t \rangle$ (see Figures 1 and 2). The exponent α clearly increases at conversions above 20%, with this effect being particularly pronounced for MMA, for which α reaches values close to unity at monomer conversions above 40% (Figure 4a). k_t^0 , on the other hand, for both MMA and DMA does not markedly change with conversion (Figure 4b). k_t^0 for MMA falls with conversion at conversions above 40%. k_t^0 values for MMA are above DMA values by about 1 order of magnitude, which is in line with the observed difference in overall $\langle k_t \rangle$ (see Figures 1 and 2). It should be noted that k_t^0 has no clear physical meaning but may be looked upon as a property of long-chain radicals extrapolated to negligible chain length. k_t^0 should definitely not be identified with experimental rate coefficients for termination reaction

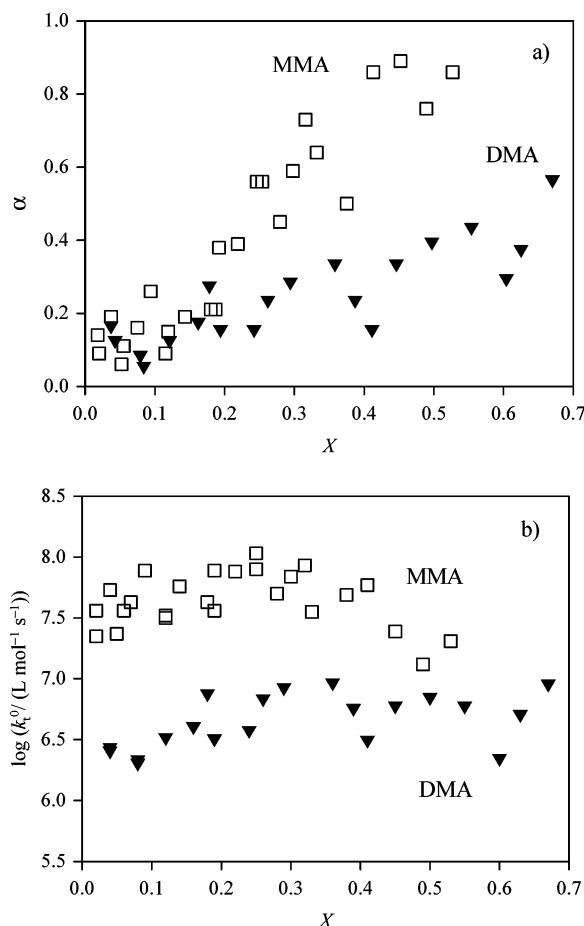


Figure 4. Fitting parameters α (a) and k_t^0 (b) plotted against monomer conversion, X , for bulk homopolymerizations of MMA at 2000 bar/40 °C (\square) and DMA at 1000 bar/40 °C (\blacktriangledown).

of two small free radicals, although the values of these two coefficients in some cases may be very close to each other. k_t^0 values will not be discussed in any detail throughout the subsequent text. It needs, however, be kept in mind that α values are strongly correlated with the corresponding k_t^0 values, as both quantities are obtained from the same fits of eq 9 to experimental SP–PLP traces. The experimental errors in k_t^0 and α values are estimated to be about 30% for both systems.

The differences in size and in conversion dependence of α at low, intermediate, and high conversions strongly suggest that different mechanisms of diffusion-control of k_t apply during the course of the polymerization reaction. At low conversions segmental diffusion with excluded-volume effects is assumed to be rate-determining, whereas center-of-mass diffusion¹⁸ controls termination in the gel-effect region. The time interval chosen for analysis of the SP–PLP traces for both monomers was $0 < t < 0.5$ s, which, under the chosen experimental p and T conditions, can be associated with the maximum free-radical chain length of about 10^4 monomer units. Immediately after the pulse all radicals are short (nonentangled), these radicals then grow to become rather long. Under gel-effect conditions, that is at higher conversions, most of these long-chain radicals become entangled.²⁴

The low-conversion MMA data presented in Figure 4a are in full agreement with literature values of $\alpha = 0.15$ (see ref 25) and $\alpha = 0.16$ – 0.17 (see ref 26). Data for higher conversions, that is, for gel-effect situations,

have not been reported so far. The low-conversion α values are also in good agreement with the theoretical value of $\alpha = 0.16$ predicted by Friedman and O'Shaughnessy²⁸ for reaction in dilute solution between long ($i > 3000$ monomer units) linear chains with radical functionality at a terminal position of each chain ("end–end" reaction). It comes as a surprise that the α value predicted for dilute solution seems to apply over an extended conversion range from zero up to monomer conversion (polymer content) of about 20%. In dilute solutions mean-field (MF) kinetics apply, and the total probability for reaction between two radicals upon their encounter may be significantly below unity due to the excluded-volume effect.²⁸ The radicals thus may get separated before termination occurs. In semidilute solutions the termination rate coefficient increases with conversion due to screening until reaction probability reaches unity. This situation would correspond to α being close to zero. However, the predictions made for semidilute and moderately concentrated regions are not supported by our experimental data: a gradual transition from the low-conversion $\alpha = 0.16$ plateau value to higher values of α for gel-effect conditions is seen. Theoretically predicted value of α for entangled polymer solutions is 1.5.^{21,27} It should be noted that our "experimental" high-conversion α values for MMA are not in conflict with such high number for α .

The values of α for methacrylates may be subdivided into two groups: (i) At low conversions, α values are close to the value of $\alpha = 0.16$, predicted for dilute solutions, and (ii) at moderately high conversions, the experiments yield relatively large α values, as are to be expected for termination via translational diffusion of entangled free radicals. It should be noted that these higher α values occur in the conversion range where also overall $\langle k_t \rangle$ significantly varies with monomer conversion (polymer concentration), which may be taken as another strong indication of translational-diffusion control of k_t under gel-effect conditions.

SP–PLP of Alkyl Acrylates. The behavior of acrylates with short alkyl ester side chains, e.g., of MA and BA, is similar to the behavior of methacrylates in that α is close to 0.16 at low conversions (Figure 5a). Toward higher conversions, α increases up to about 0.4 for MA and up to about 0.3 for BA. α for DA, on the other hand, is relatively high from the very beginning of the polymerization reaction. Another interesting observation is that, while α values for MA and BA are close to each other at low conversion, α values for MA and DA closely approach each other at moderately high degrees of monomer conversion and are distinctly above high-conversion α values for BA. This unexpected variation results in the surprising sequence of α values at moderate conversions around 30%, where α increases from BA to MA and to DA, thus showing no systematic variation with the size of the alkyl ester group. As can be seen from Figure 5b, the associated k_t^0 values for the three alkyl acrylate monomers exhibit no significant dependence on monomer conversion (Figure 5b). As with methacrylates, the experimental errors in k_t^0 and α values are estimated to be about 30%.

A previously reported value for methyl acrylate at low conversion is $\alpha = 0.32$ (see ref 13). The difference between this value and the values given in Figure 5a probably results from the fact that the fitting procedure in ref 13 was carried out with k_t^0 being fixed at 7×10^8 $\text{L mol}^{-1} \text{s}^{-1}$, whereas the fitting procedure of the present

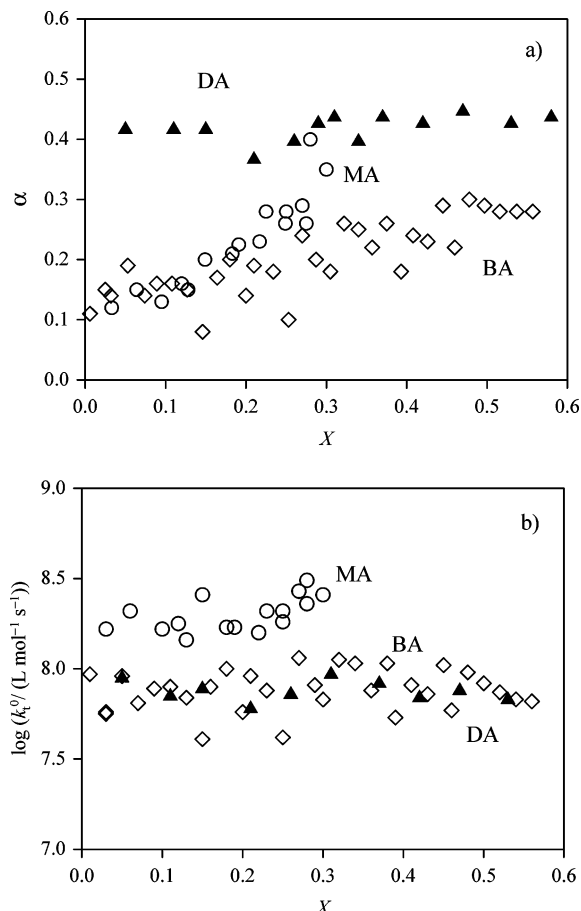


Figure 5. Fitting parameters α (a) and k_t^0 (b) plotted against monomer conversion, X , for bulk homopolymerizations of MA (○), BA (◇), and DMA (▲) at 1000 bar and 40 °C.

study yields k_t^0 of around $2 \times 10^8 \text{ L mol}^{-1} \text{ s}^{-1}$ (Figure 5b, Table 1). Adopting the k_t^0 value from ref 13 for the analysis of the present SP–PLP data, one obtains low-conversion α values which are close to the literature value of 0.32.

The low-conversion α values for MA and BA (and for MMA and DMA) are in almost perfect agreement with the theoretical value of $\alpha = 0.16$ predicted by Friedman and O'Shaughnessy.²⁸ Toward higher monomer conversion α increases, although to a weaker extent than with methacrylates (see Figure 4a). This difference may be understood as resulting from a significantly weaker gel effect in the case of acrylates. As is to be expected,²⁹ the gel effect is stronger for MA than for BA, which is associated with α being larger for MA than for BA in the region of translation-diffusion control of termination.

The arguments presented so far do not explain why α values for DA are so high from the very beginning of the polymerization reaction. For dilute polymer solutions, Friedman and O'Shaughnessy²⁸ predicted α to be above 0.16 for reactions where the active site of at least one free radical is located somewhere along the backbone, which species is referred to as "midchain" radical. For reaction of such a "midchain" radical with an end-functional free radical, an "end-interior" reaction, α is predicted to be 0.27, and for the reaction of two "midchain" free radicals α should be as high as 0.43. Thus, it appears tempting to assume that the α values for DA are indicative of strong contributions of "midchain" radicals to termination.

"Midchain" radicals may be produced by inter- and intramolecular chain-transfer processes. As the high α value for DA is already seen at very low conversion where only small amounts of polymer are present, intramolecular chain transfer must play an important role. In principle, intramolecular chain transfer from a terminal site may occur to any position at the macro-radical. Backbiting via a six-membered ring is a particularly well-known special type of intramolecular chain transfer which accounts for a significant fraction of butyl side chains in ethene high-pressure high-temperature polymerization. There is also strong literature evidence for the occurrence of intramolecular chain transfer in acrylate polymerizations.²⁹ For acrylates with large alkyl ester side group, Scott and Senogles reported that the dependence of polymerization rate, r_p , on initiation rate, r_i , and monomer concentration follows the rate law:

$$r_p \propto (r_i)^\alpha (c_M)^\beta, \quad \alpha < 0.5, \quad \beta \approx 1.5$$

which observation may be understood as being due to significant intramolecular chain transfer.

During recent years, overwhelming evidence for intramolecular chain transfer in acrylate free-radical polymerization has been provided, chiefly by the groups of Lovell,³⁰ Asua,³¹ and Yamada.³² The occurrence of fairly high "midchain" radical concentrations is also favored by the much slower propagation rate of the tertiary free radicals produced by the chain-transfer process. By intramolecular chain transfer already at low conversions, significant concentrations of "midchain" radicals may be generated. If "midchain" radicals actually are responsible for the large α value for DA, it is, however, not easily understood why low-conversion α for MA and BA is smaller. (Backbiting with these two monomers should be at least as efficient as with DA.) A tentative explanation for the different sizes of low-conversion α could be that it is not only and not primarily backbiting which produces "midchain" radicals and that chain transfer may occur to any site of the macroradical. If this is true, acrylates with long alkyl ester chains should provide particularly favorable conditions for such intramolecular chain transfer as they offer a large amount of hydrogen atoms to be abstracted.

To test this hypothesis, SP–PLP experiments have been carried out on two other acrylates with longer alkyl ester side chain, *n*-hexyl acrylate (HA) and 2-ethylhexyl acrylate (EHA). As can be seen from Figure 6, α values for both monomers are well above 0.16: $\alpha(\text{HA})$ is close to 0.3, and $\alpha(\text{EHA})$ is already very close to the DA α value. Moreover, the EHA data also show no detectable conversion dependence of α as do the DA data. The data in Figure 6 are not in conflict with the assumption that alkyl acrylates with ester side groups larger than butyl readily undergo intramolecular chain transfer to yield "midchain" radicals.

As a further test of the hypothesis that conversion-independent α values above 0.16 reflect "midchain" radicals being brought upon by intramolecular chain transfer, a few SP–PLP experiments have been carried out on mixtures of BA and of DA with supercritical carbon dioxide (scCO₂). Polymerization in solution at otherwise identical conditions should enhance the formation of "midchain" radicals, as intramolecular chain transfer will be favored by the larger mobility of chain

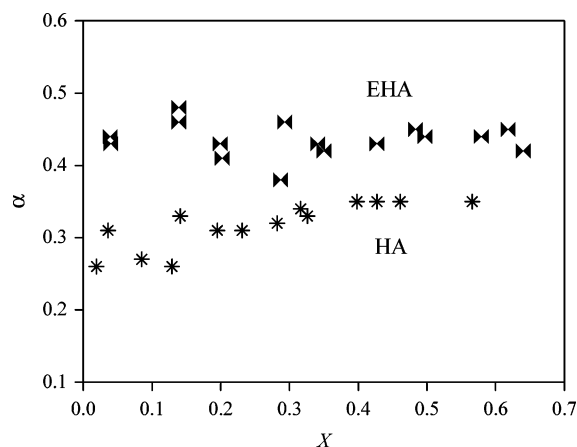


Figure 6. Variation of α with monomer conversion, X , for bulk homopolymerizations of *n*-hexyl acrylate, HA (*), and 2-ethylhexyl acrylate, EHA (○), at 1000 bar and 40 °C. The values of α were obtained by fitting eq 9 to SP–PLP data.

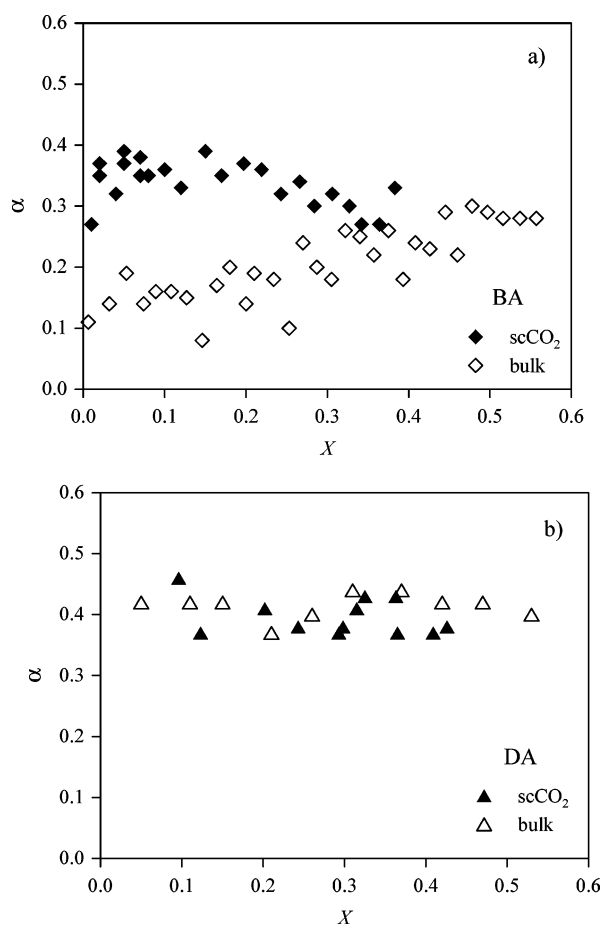


Figure 7. Exponent α plotted against monomer conversion, X , for SP–PLP of (a) BA in bulk (◇) and in mixtures with 40 wt % of $scCO_2$ (◆) and (b) DA in bulk (△) and in mixtures with 40 wt % of $scCO_2$ (▲) carried out at 1000 bar and 40 °C.

segments and by the reduced propagation rate of free radicals. $scCO_2$ is a particularly interesting solvent because the advantage of lowering propagation rate by dilution is not counterbalanced by the disadvantage of transfer reaction to the solvent, as CO_2 has zero transfer activity. For this reason, CO_2 has been frequently used as a solvent in free-radical polymerizations during recent years.^{33,34}

The results of SP–PLP studies into α for BA and DA polymerized in bulk and in mixtures with $scCO_2$ are

plotted in parts a and b of Figure 7, respectively. For BA a large difference between α 's for bulk and for solution polymerizations is seen, whereas with DA the bulk and solution α 's are identical within the limits of experimental accuracy. These findings may be understood as follows: During bulk polymerization of BA (at 40 °C and 1000 bar) the concentration of "midchain" radicals is not sufficiently high to give rise to α values well above 0.16. With 40 wt % CO_2 being present, however, the fraction of "midchain" radicals is increased to such an extent that low-conversion α reaches values of about 0.35. With DA, where the concentration of "midchain" radicals appears to be sufficiently high even in bulk polymerization, methods of further enhancing this concentration, e.g., by carrying out SP–PLP experiments on solutions containing CO_2 , are not expected to have an influence on α . This is indeed what is observed.

5. Conclusions

The analysis of SP–PLP data for several alkyl acrylates and alkyl methacrylates clearly shows that k_t is chain-length-dependent at both low and high degrees of monomer conversion. The chain-length dependence (CLD) of k_t is particularly strong for methyl acrylates under gel-effect conditions. Also for alkyl acrylates with large alkyl ester group, such as dodecyl acrylate or 2-ethylhexyl acrylate, k_t changes markedly with chain length. At present, the signal quality of SP–PLP experiments is not sufficiently high to allow for discrimination between different models for CLD of k_t . The analysis of SP–PLP data thus has been carried out by adopting the validity of the simple power-law model $k_{t(i,j)} = k_t^0 i^{-\alpha}$.

Three types of α behavior are seen: (i) At low degrees of monomer conversions, typically up to 20%, α is close to the theoretically predicted value of 0.16, which number holds for macroradicals with terminal free-radical functionality as are occurring in polymerizations of the methacrylates and also seem to occur for alkyl acrylates with small alkyl ester group. (ii) At higher concentrations of methacrylates (and alkyl acrylates with small alkyl ester group), in particular under gel-effect conditions, where termination is controlled by translation diffusion, α may be significantly above 0.16 and may even approach unity, as is the case with MMA. (iii) Relatively high α is found for acrylates with larger alkyl ester groups throughout their entire monomer conversion range. This effect is assigned to termination predominantly taking place between "midchain" radicals, for which reaction theory predicts α of 0.43.

The "midchain" radicals are produced by intramolecular chain-transfer processes. SP–PLP experiments on alkyl acrylate– CO_2 mixtures support the assumption that "midchain" radical termination is responsible for the observed high α values, e.g., in DA polymerization. Within ongoing work, the branching structure of the polymeric products will be analyzed in detail. Moreover, SP–PLP measurements will be carried out at lower temperatures where chain-transfer processes should be less important.

Acknowledgment. Financial support by the Deutsche Forschungsgemeinschaft (DFG) through the European Graduate School "Microstructural Control in Free-Radical Polymerization" and the Graduate School 782 "Spectroscopy and Dynamics of Molecular Aggregates, Chains, Clusters and Networks" is gratefully

acknowledged as is the support by the Fonds der Chemischen Industrie.

References and Notes

- (1) Buback, M.; Gilbert, R. G.; Russell, G. T.; Hill, D. J. T.; Moad, G.; O'Driscoll, K. F.; Shen, J.; Winnik, M. A. *J. Polym. Sci., Polym. Chem. Ed.* **1992**, *30*, 851.
- (2) Olaj, O. F.; Bitai, I.; Hinkelmann, F. *Makromol. Chem.* **1987**, *188*, 1689. Olaj, O. F.; Schnöll-Bitai, I. *Eur. Polym. J.* **1989**, *25*, 635. Beuermann, S.; Buback, M. *Prog. Polym. Sci.* **2002**, *27*, 191.
- (3) Buback, M.; Gilbert, R. G.; Hutchinson, R. A.; Klumperman, B.; Kuchta, F.-D.; Manders, B. G.; O'Driscoll, K. F.; Russell, G. T.; Schweer, J. *Macromol. Chem. Phys.* **1995**, *196*, 3267. Beuermann, S.; Buback, M.; Davis, T. P.; Gilbert, R. G.; Hutchinson, R. A.; Olaj, O. F.; Russell, G. T.; Schweer, J.; van Herk, A. M. *Macromol. Chem. Phys.* **1997**, *198*, 1545.
- (4) Buback, M.; Egorov, M.; Kaminsky, V.; Olaj, O. F.; Russell, G. T.; Vana, P.; Zifferer, G. *Macromol. Chem. Phys.* **2002**, *203*, 2570.
- (5) Russell, G. T.; et al. To be submitted to *Macromol. Chem. Phys.*
- (6) Buback, M.; Hippler, H.; Schweer, J.; Vögele, H.-P. *Makromol. Chem. Rapid Commun.* **1986**, *7*, 261.
- (7) Buback, M.; Kowollik, C. *Macromolecules* **1999**, *32*, 1445.
- (8) Buback, M.; Feldermann, A. *Aust. J. Chem.* **2002**, *55*, 475.
- (9) Beuermann, S.; Buback, M.; Schmaltz, C. *Ind. Eng. Chem. Res.* **1999**, *38*, 3338.
- (10) Buback, M.; Barner-Kowollik, C.; Egorov, M.; Kaminsky, V. *Macromol. Theory Simul.* **2001**, *10*, 209.
- (11) Vana, P.; Davis, T. P.; Barner-Kowollik, C. *Aust. J. Chem.* **2002**, *55*, 315.
- (12) Fischer, H.; Baer, R.; Hany, R.; Verhoolen, I.; Walbinder, M. *J. Chem. Soc., Perkin Trans.* **1990**, *2*, 787.
- (13) Buback, M.; Busch, M.; Kowollik, C. *Macromol. Theory Simul.* **2000**, *9*, 442. Kowollik, C. Ph.D. Thesis, Göttingen, 1999.
- (14) Vana, P.; Davis, T. P.; Barner-Kowollik, C. *J. Polym. Sci., Polym. Chem. Ed.* **2002**, *40*, 675.
- (15) Buback, M.; Egorov, M.; Feldermann, A. *ACS Symp. Ser.* **2002**, *854*, 42.
- (16) Buback, M.; Kowollik, C. *Macromolecules* **1998**, *31*, 3221.
- (17) De Kock, J. B. L.; Van Herk, A. M.; German, A. L. *J. Macromol. Sci., Polym. Rev.* **2001**, *C41* (3), 199.
- (18) Soh, S. K.; Sundberg, D. C. *J. Polym. Sci., Polym. Chem. Ed.* **1982**, *20*, 1299, 1315, 1331, 1345. Russell, G. T.; Napper, D. H.; Gilbert, R. G. *Macromolecules* **1988**, *21*, 2133, 2141.
- Buback, M. *Macromol. Chem. Phys.* **1990**, *191*, 1575.
- (19) Olaj, O. F.; Zifferer, G.; Gleixner, G. *Macromol. Chem., Rapid Commun.* **1985**, *6*, 773. Olaj, O. F.; Zifferer, G.; Gleixner, G. *Macromol. Chem.* **1986**, *187*, 977. Olaj, O. F.; Zifferer, G.; Gleixner, G. *Macromolecules* **1987**, *20*, 839.
- (20) Nikitin, A. N.; Evseev, A. V. *Macromol. Theory Simul.* **1997**, *6*, 1191.
- (21) De Gennes, P. G. *J. Chem. Phys.* **1982**, *76*, 3316, 3322.
- (22) For the termination model represented by eq 10, eq 12 can be integrated to yield an analytical expression for $c_M(t)/c_M^0$ (not given here).
- (23) χ^2 is defined as the sum of the squares of the deviations of the theoretical curve(s) from experimental points.
- (24) The entanglement length, i_e , can be estimated using e.g. the scaling relationship of de Gennes: $i_e = i_{e0}/\phi_p^2$, where $i_{e0} \cong 100$ and ϕ_p is polymer volume fraction. Or, approximately, $i_e = i_{e0}/x^2$, where x is monomer conversion. At 20% conversion, therefore, $i_e \cong 2500$, which is just within the range of radical lengths under investigation.
- (25) Mahabadi, H. K. *Macromolecules* **1985**, *18*, 1319.
- (26) Olaj, O. F.; Vana, P. *Macromol. Chem., Rapid Commun.* **1998**, *19*, 433, 533.
- (27) Doi, M.; Edwards, S. F. *J. Chem. Soc., Faraday Trans. 1* **1978**, *78*, 1789. Doi, M.; Edwards, S. F. *The Theory of Polymer Dynamics*; Oxford University Press: New York, 1986.
- (28) Friedman, B.; O'Shaughnessy, B. *Macromolecules* **1993**, *26*, 5726. Karatekin, E.; O'Shaughnessy, B.; Turro, N. J. *Macromol. Symp.* **2002**, *182*, 81.
- (29) Scott, G. E.; Senogles, E. *J. Macromol. Sci., Chem.* **1970**, *A4*, 1105. Scott, G. E.; Senogles, E. *J. Macromol. Sci., Chem.* **1974**, *A8*, 753.
- (30) Britton, D.; Heatley, F.; Lovell, P. A. *Macromolecules* **1998**, *31*, 2828. Ahmad, N. M.; Heatley, F.; Lovell, P. A. *Macromolecules* **1998**, *31*, 2822.
- (31) Plessis, Ch.; Arzamendi, G.; Alberdi, J. M.; van Herk, A. M.; Leiza, J. R.; Asua, J. M. *Macromol. Rapid Commun.* **2003**, *24*, 173. Plessis, Ch.; Arzamendi, G.; Leiza, J. R.; Schoonbrood, H. A. S.; Charmot, D.; Asua, J. M. *Macromolecules* **2000**, *33*, 4.
- (32) Azukizawa, M.; Yamada, B.; Hill, D. J. T.; Pomery, P. J. *Macromol. Chem. Phys.* **2000**, *201*, 774.
- (33) Beuermann, S.; Buback, M.; Kuchta, F.-D.; Schmaltz, C. *Macromol. Chem. Phys.* **1998**, *199*, 1209.
- (34) Beuermann, S.; Buback, M.; El Rezzi, V.; Jürgens, M.; Nelke, D. *Macromol. Chem. Phys.* Submitted.

MA0350922